Research Journal of Applied Sciences, Engineering and Technology 7(18): 3916-3925, 2014
DOI:10.19026/rjaset.7.750
ISSN: 2040-7459; e-ISSN: 2040-746

Submitted: December 18, 2013 Accepted: December 27, 2013 Published: May 10, 2014

Research Article

Modeling and Multi-response Optimization of Hard Milling Process using Desirability Function Approach

A. Tamilarasan and K. Marimuthu
Department of Mechanical Engineering, Coimbatore Institute of Technology,
Civil Aerodrome Post, Coimbatore-641014, Tamilnadu, India

Abstract: The characteristic features of hard milling are variable chip thickness and intermittent cutting. Such tendency rapidly increases the tool wear and reduces the metal removal rate against the cutting temperature results poor surface finish. Therefore, the objective of this present study was to present the mathematical models for modeling and analysis on the effects of process parameters, including the feed per tooth, radial depth of cut, axial depth of cut and cutting speed on cutting temperature, tool wear and metal removal rate in hard milling of 100MnCrW4 (Type O1) tool steel using (TiN+TiAlN) coated carbide inserts. A central composite rotatable design with four factors and five levels was chosen to minimize the number of experimental conditions. Further, the reduced developed models were used for multiple-response optimization by desirability function approach in order to determine the optimum cutting parameters. These optimized machining parameters are validated experimentally and the experimental and predicted values were in a good agreement with small consistent error.

Keywords: Central composite design, cutting temperature, desirability function, hard milling, metal removal rate, tool wear

INTRODUCTION

Hard milling is a promising green technology in the manufacturing of precision components from hardened (40 HRC and more) tool steels (Ding *et al*., 2010). Reliable hard milling process is a key to reduce many numbers of a process chain in the manufacturing sectors (Davim, 2011). The prime advantages are improve productivity, reduced increased flexibility, decreased capital expenses and reduced environmental hazards with regards to traditional route, which involves processes such as annealing, heat treatment, grinding or electrical discharge machining and manual finishing (Gopalsamy *et al*., 2010). The main limitation on the other side is high-heat generation in the cutting zone makes rapid tool wear as compared with conventional milling. The cutting temperature is dominating a surface finish and severe tool wear sweeps less volume of metal removal. Many research studies have been conducted to investigate the performance of coated WC and CBN tools in hard milling of various hardened materials. Ghani *et al*. (2004) found that the early crack initiates at the cutting edge due to high mechanical impact caused by the combined effect of high depth of cut and feed rate in semi-finishing and finishing end milling of hardened AISI H13 tool steel (50±3 HRC) at high cutting speed regime. The resulting tool life is highly affected by feed rate and depth of cut. However, the effect of cutting speed is less significant. Okada *et al*. (2011) evaluated a tool wear, cutting temperature, cutting forces and surface roughness in hard milling of JIS S55C carbon steel with different hardness range using CBN and coated WC inserts. They found that CBN and TiAlN/AlCrN coated carbide tools produce very fewer tool wears. Mativenga and Hon (2005) performed a cutting test at a very high speed around 40000 RPM to understanding the effect of various coated carbide tools in machining of H13 tool steel (50 HRC). They suggest that TiAlN coated tools outperformed well and great potential for HSM conditions. Toh (2005) observed that irrespective of milling orientation the chip surface temperature increased in all axial depth of cut with increased tool flank wear. In addition, the cutter condition also considerably increasing the chip surface temperature. Siller *et al*. (2009) revealed the surface finish of 0.1 to 0.3 μm with acceptable tool life in face milling of AISI D3 tool steel (60 HRC) using different geometric features of PVD based AlCrN coated carbide tools. The special features of chamfer preparation, cutting angle's design and radii combinations were used for process viability in finishing of hardened mold and die components. Escalona *et al*. (2012) showed different tool wear mechanisms for the cutting speed range of 150 to 1250 m/min in face milling of 1045 steel. The abrasion, adhesion, diffusion, mechanical

Corresponding Author: A. Tamilarasan, Department of Mechanical Engineering, Coimbatore Institute of Technology, Civil Aerodrome Post, Coimbatore-641014, Tamilnadu, India

fatigue and thermal fatigue mechanisms were observed for different ranges of cutting speed. The feed per tooth has the most influence on the critical cutting speed, followed by the cutting time and finally, the axial depth of cut. The tool flank wear was influenced by in the order of cutting speed, feed per tooth and axial depth of cut. Sato *et al*. (2007) used two-color pyrometer to measure the tool-chip interface temperature in end milling. They found that down milling produces the maximum tool temperature about 50°C higher than that in up milling and when the cutting speed is doubled the temperature difference in rake face is about 90°C was observed. Gu *et al*. (1999) studied the flank wear of uncoated and different coated tools in face milling of 4140 preheat treated steel. During cutting, the TiAlN coating produces higher wear resistance, followed by TiN coating and ZrN coating. The TiAlN and TiN coatings reduce the BUE wear at low cutting speeds and produce a lower wear rate at high cutting speeds due to low thermal conductivity. The micro-attrition, micro-abrasion, mechanical fatigue, thermal fatigue and chipping were observed in uncoated inserts as a function of feed rate and cutting speed. For coated inserts, abrasive wear was found in the coating and attrition; micro-attrition or micro-abrasion was found in exposed substrate. Cui *et al*. (2012) conducted experiments and finite-element simulations on high-speed hard milling of H13 tool steel (47-47 HRC) using Ti (C, N) -Al_2O_3 coated carbide inserts. The cutting speed was utilized in the range of 200 to 2400 m/min. The low averaged resultant cutting force with long tool life was observed in the critical cutting speed of 140 m/min. The higher cutting force, tool temperature, mechanical impact and thermal impact may lead the severe tool wear. It is understood from the literatures that in various research directions, the hard milling process were analyzed. In the current study aims to use, the hard milling indices are of cutting temperature, tool wear and metal removal rate as multi responses, as an effective method for finding the optimal cutting conditions for hard milling of 100MnCrW4 (Type O1) cold work tool steel using (TiN+TiAlN) coated carbide inserts using RSM with desirability function.

METHODOLOGY

Response surface methodology with desirability function: Response surface methodology is a widely practiced approach for various fields, particularly in situations where several input variables influence a quality characteristic of the product or process. The most popular class of second-order designs called Central Composite Design (CCD) was used for RSM in the experimental design. The CCD is well suited for fitting a quadratic surface, which usually works well for the process optimization (Montgomery, 2012). Commonly, a quadratic response surface model with cross terms can be constructed to fit the experimental data obtained in accordance with CCD. The response surface model, known also as regression or empirical equation, represents a polynomial approximation to experimental data and is stated by the following relationship:

$$y = \beta_0 + \sum_{i=1}^{k} \beta_i x_i + \sum_{i=1}^{k} \beta_{ii} x_i^2 + \sum_{i} \sum_{j} \beta_{ij} x_i x_j + \varepsilon \quad (1)$$

where,
y = The desired response
x_i = The values of the i^{th} hard milling parameters
β_0 = The model constant
β_i = The linear coefficient
β_{ii} = Denotes the quadratic coefficient
β_{ij} = The interaction coefficient
k = The number of the factors or variables
ε = The statistical experimental error

The empirical relations were developed to predict all the responses and the more popular statistical procedure of Analysis of Variance (ANOVA) is adopted to justify the significance of the developed empirical models. Further, there is a necessity to locate the region of required goals of responses reside within the experimental domain. Derringer and Suich (1980) proposed one useful approach for the optimization of multiple responses is to use the simultaneous optimization technique called desirability. The method makes use of an objective function, D, called the desirability function and transforms an estimated response into a scale-free value (d_i) called desirability. The desirable ranges are from zero to one (least to most desirable, respectively). The factor settings with maximum total desirability are considered to be the optimal parameter conditions. The simultaneous objective function is a geometric mean of all transformed responses:

$$D = \left[\prod_{i=1}^{m} d_i\right]^{\frac{1}{m}} \quad (2)$$

where, m is the number of responses in the measure. If any of the responses fall outside the desirable range, the overall function becomes zero. Besides, a confirmatory experiment was carried out to verify the optimal setting of cutting conditions.

Hard milling experiments:

Experimental design: A central composite experimental design used for response surface modeling of hard milling process and was carried out using four independent process variables, namely, the following: feed per tooth (f_z), radial depth of cut (a_e), axial depth of cut (a_p) and cutting speed (V_c) were selected based on preliminary experiments and literature survey. The prime advantage of CCD is efficient and flexible, providing sufficient information about the effects of variables and overall experimental error with a

Table 1: Hard milling parameters and their levels

Parameters	Labels	Levels				
		-2	-1	0	+1	+2
Feed per tooth (f_z)	A	0.05	0.1	0.15	0.20	0.25
Radial depth of cut (a_e)	B	0.20	0.3	0.40	0.50	0.60
Axial depth of cut (a_p)	C	0.20	0.4	0.60	0.80	1.00
Cutting speed (V_c)	D	200	250	300	350	400

Fig. 1: Hard milling experimental setup

minimum number of experiments (Montgomery, 2012). Therefore, a central composite design with four factors at five levels was conducted in the present work. Thirty experiments were augmented with six replications at the center point to evaluate the pure error. Table 1 shows the hard milling parameters and their levels. For statistical calculations, the variables X_i were coded as x_i according to the following empirical relationship:

$$x_i = \frac{X_i - X_0}{\delta X} \quad (3)$$

where,
X_0 = The value of the X_i at the center point
δX = The step change

Experimental work: The machining trials were carried out at the CNC vertical machining center (MAZAK-NEXUS 510C-II) with a maximum spindle speed of 12000 rpm, a power output of 25 HP and a capability to employ feed rates up to 36 m/min The tool steel blocks are of final dimensions 150×150×25 mm were prepared after heat treatment and corresponding compositions are 0.95% C; 1.1% Mn; 0.6% Cr; 0.6% W; 0.25% Si; 0.03 P; 0.01% S; 0.1% Mo. The typical uses are making dies and molds, punches, master tools and precision gauges. The work-pieces were quenched in oil from the austenitising temperature and were double tempered. Different tempering cycles were employed in the steel to obtain the hardness of 50 HRC (ASM Handbook, 1991). A Taegutec tool holder (2S-TE90AP 320-W20-09) and TT9080 grade (APKT 09T320R-EM) carbide inserts were selected for the present work. The hard milling experimental setup is shown in Fig. 1. The experiments were conducted in a random fashion as per the CCD design matrix of 'RUN' column and total cutting pass kept 300 mm length. For each cutting condition, the values of tool flank wear of all tools were measured with an optical microscope and were examined using Scanning Electron Microscopy (SEM) (JSM-6510LV, Japan) and Energy-Dispersive X-ray Spectroscopy (EDS) to understand the various wear mechanisms in tool and chip morphology. Further, the tool flank wear was measured three times for each insert in accordance with ISO 8688-1989 standard and the average value was taken for analysis. A non-contact fluke type (Type 8839) pyrometer was utilized to capture the maximum cutting temperature during machining. Figure 2 depicts that a single-point laser beam was focused to capture noticeable temperature at tool-chip interface zone (Cydas, 2010) by adjusting the

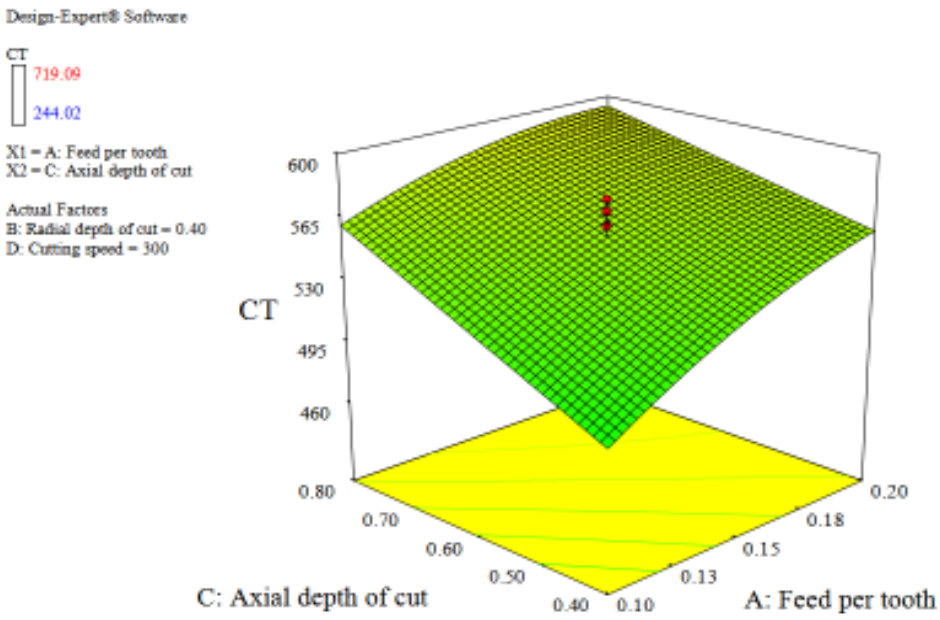

Fig. 2: 3D surface plot for CT

Table 2: CCD design matrix with responses

		Factors				Responses		
Std	Run	A mm/z	B mm	C mm	D m/min	CT °C	TW mm	MRR g/min
1	2	0.10	0.30	0.40	250	334.09	0.107	1.196
2	17	0.20	0.30	0.40	250	407.01	0.183	2.282
3	22	0.10	0.50	0.40	250	349.57	0.113	2.027
4	25	0.20	0.50	0.40	250	378.68	0.191	4.055
5	26	0.10	0.30	0.80	250	419.04	0.125	2.433
6	3	0.20	0.30	0.80	250	441.52	0.195	4.866
7	19	0.10	0.50	0.80	250	438.82	0.129	4.355
8	21	0.20	0.50	0.80	250	460.71	0.201	7.981
9	8	0.10	0.30	0.40	350	575.26	0.135	2.696
10	28	0.20	0.30	0.40	350	650.84	0.209	3.885
11	18	0.10	0.50	0.40	350	609.02	0.139	3.237
12	5	0.20	0.50	0.40	350	693.78	0.213	6.175
13	10	0.10	0.30	0.80	350	600.35	0.144	3.085
14	30	0.20	0.30	0.80	350	673.63	0.210	7.770
15	29	0.10	0.50	0.80	350	696.61	0.153	6.475
16	24	0.20	0.50	0.80	350	705.47	0.219	9.640
17	11	0.05	0.40	0.60	300	469.66	0.093	1.696
18	16	0.25	0.40	0.60	300	575.46	0.243	7.348
19	14	0.15	0.20	0.60	300	505.20	0.169	2.674
20	15	0.15	0.60	0.60	300	546.17	0.187	7.581
21	9	0.15	0.40	0.20	300	491.55	0.175	2.178
22	6	0.15	0.40	1.00	300	591.67	0.199	8.424
23	12	0.15	0.40	0.60	200	244.02	0.112	1.088
24	27	0.15	0.40	0.60	400	719.09	0.152	5.241
25	13	0.15	0.40	0.60	300	560.73	0.148	5.038
26	7	0.15	0.40	0.60	300	559.81	0.142	4.930
27	4	0.15	0.40	0.60	300	567.64	0.148	5.865
28	23	0.15	0.40	0.60	300	574.94	0.143	4.664
29	1	0.15	0.40	0.60	300	552.28	0.145	5.554
30	20	0.15	0.40	0.60	300	568.37	0.142	5.839

emissivity value of 0.8 for this work-piece. The measuring range of a pyrometer is -50 to 1000°C with an accuracy of ±2°C. The temperatures were calculated for a maximum of fifteen peak points for each run and three replicates were considered. In all the experiments, the machining time was noted at the end of each 300 mm cutting length and loss of weight method was used to calculate the metal removal rate. For each experiment, the work-piece weight was measured using a digital balance with 0.001 mm accuracy. The experiments were triplicate and each experiment response for all the experiments was listed in Table 2.

RESULTS AND DISCUSSION

The mathematical model for CT, TW and MRR: Based on experimental design results the regression models have been developed using DESIGN EXPERT software in order to determine the functional relationship for approximation and prediction of responses. Thus, the final second-order models with un-coded variables obtained in hard milling process are as follows:

$$CT\ (°C) = -1207.1727 + 1996.746429 \times A + 55.7226 \times B + 529.527 \times C + 6.51711 \times D - 849.125 \times AC + 2.2335 \times BD - 0.897375 \times CD - 3289.571429 \times A^2 - 744.2678571 \times B^2 - 0.00739 \times D^2 \quad (4)$$

$$TW\ (\mu m) = + 0.06604 + 0.1275 \times A - 0.635833 \times B - 0.21645 \times C + 0.0010575 \times D - 0.175 \times AC - 0.0001625 \times CD + 2.3583 \times A^2 + 0.8395 \times B^2 + 0.266145833 \times C^2 - 0.000001241 \times D^2 \quad (5)$$

$$MRR\ (g/min) = - 26.331 + 25.3575 \times A + 1.5279 \times B - 5.3404 \times C + 0.14648 \times D + 41.675 \times AC + 15.19375 \times BC - 77.725 \times A^2 - 0.000213475 \times D^2 \quad (6)$$

Statistical analysis: Statistical results were obtained from the Analysis of Variance (ANOVA) for the validity of the final quadratic models is shown in Table 3. The ANOVA table summarizes the sum of squares of residuals and regressions together with the corresponding degrees of freedom, F-values and ANOVA coefficients (i.e., coefficients of multiple determination R^2 and adjusted R^2 statistics for each empirical model corresponding to each response). As can be seen, the coefficients of determination (R^2) of each response were 98.96, 99.75 and 96.97%, respectively which guarantee high validity of the regression functions. Furthermore, these values indicate that more than 98.96% for CT, 99.75% for TW and 96.97% for MRR of the data deviation can be explained by the each empirical model. The value of 'Prob>F' for models is less than 0.05, indicated that the model is significant, which is desirable as it indicates that the terms to the model have a significant effect upon the response. The models F-values of 180.45, 755.8774383

Table 3: ANOVA table for the fitted models

Source	S.S.	df	M.S.	F	Prob>F	
For CT						
Model	408300	10	40828.21	180.45	<0.0001	Significant
Residual	4298.96000	19	226.26			
Lack of fit	3981.33000	14	284.38	4.48	0.0537	Not significant
Pure error	317.63000	5	63.53			
Cor total	412600	29				
Std dev	15.04200			R^2	0.9896	
Mean	532.03300			Adjusted R^2	0.9841	
C.V.%	2.82726			Pred R^2	0.9728	
PRESS	11217.62000			Adeq precision	53.5340	
For TW						
Model	0.04167272	10	0.00416727	755.8774383000	<0.0001	Significant
Residual	0.00010475	19	5.5132E-06			
Lack of fit	0.00006542	14	4.6726E-06	0.593976998	0.7968	Not significant
Pure error	0.00003933	5	7.8667E-06			
Cor total	0.04177747	29				
Std dev	0.00234801			R^2	0.9975	
Mean	0.16213333			Adjusted R^2	0.9962	
C.V.%	1.44819787			Pred R^2	0.9933	
PRESS	0.00027793			Adeq precision	102.6900	
For MRR						
Model	151.14633250	8	18.8932916	84.106440140	<0.0001	Significant
Residual	4.71734530	21	0.22463549			
Lack of fit	3.43439330	16	0.21464958	0.836545651	0.6449	Not significant
Pure error	1.28295200	5	0.2565904			
Cor total	155.86368000	29				
Std dev	0.47395730			R^2	0.9697	
Mean	4.67593330			Adjusted R^2	0.9582	
C.V.%	10.13610000			Pred R^2	0.9400	
PRESS	9.35942670			Adeq precision	36.4730	

and 84.10644014 imply the models are significant. The value of $p<0.0001$ indicates that there is only a 0.01% chance that a 'model F-value' this large could occur due to noise. In this case, for CT (A, B, C, D, AC, BD, CD, A^2, B^2 and D^2), for TW (A, B, C, D, AC, CD, A^2, B^2, C^2 and D^2), for MRR (A, B, C, D, AC, BC, A^2 and D^2) are significant model terms. The insignificant model terms can be removed and may result in an improved model. The 'Lack of Fit F-value' for CT = 0.0537, TW = 0.7968 and MRR = 0.6449 imply the Lack of Fit is not significant relative to the pure error. There is a 180.45, 755.8774383 and 84.10644014%, respectively chance that a 'Lack of Fit F-value' this large could occur due to noise for CT, TW and MRR. Insignificant lack of fit is good as sufficiently good model fitting is desirable. Moreover, for all responses the predicted R^2 values are in agreement with the Adjusted R^2 values. This means that significant terms have been included in all empirical models. The adequate precision value is an index of the signal-to-noise ratio; value of more than 4 is desirable. For all models, the adequate precision values were greater than 35. The statements are leading to a conclusion that the developed models were a good fit.

The effect of process parameters on cutting temperature: The Fig. 2 illustrates the interaction between axial depth of cut and feed rate per tooth on cutting temperature for the fixed factors of radial depth of cut (0.40 mm) and cutting speed (225 m/min) at the middle level. The CT was raised by the increase of feed per tooth and axial depth of cut for all ranges of conditions. It seems that increase of chip volume causes more power consumption for plastic shearing of metal to form the chips. Due to high power consumption, the great rate of mechanical energy from cutting forces converted into heat and high cutting temperature near the cutting edge on the tool (Palanisamy *et al*., 2006; El-Wardany *et al*., 2000). The cutting temperature varies by the type of material being machined and cutting conditions. It can be observed in the SEM (Fig. 3), the presence of fissures was generated due to the cutting temperature and mechanical load were involved in during the hard milling process. These fissures are characteristics of a worn tool involved in a thermal fatigue tool wear mechanism (Escalona *et al*., 2012).

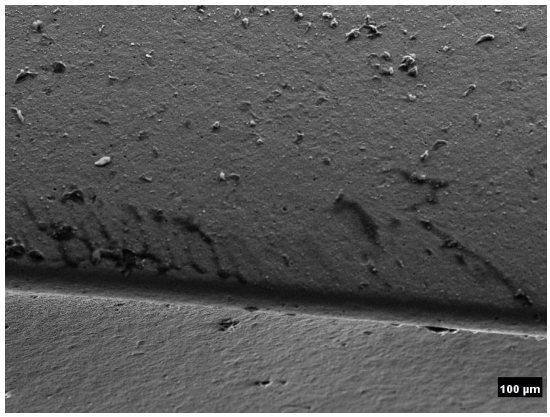

Fig. 3: SEM picture on tool rake face

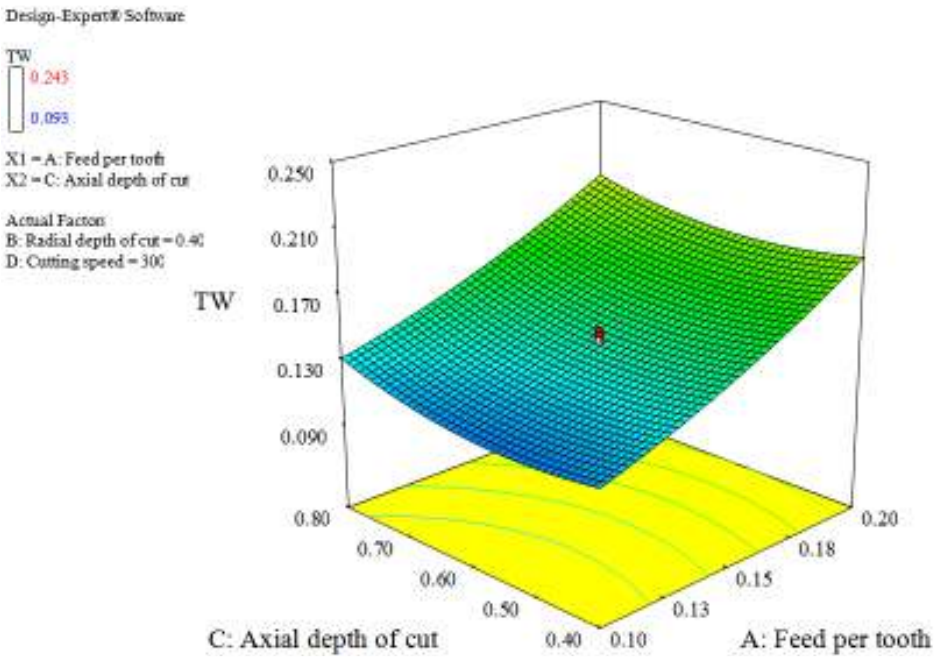

Fig. 4: 3D surface plot for TW

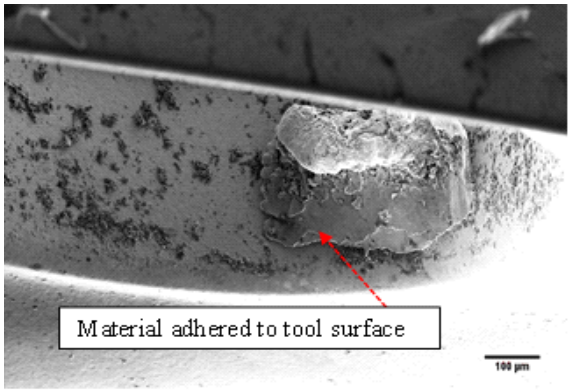

Fig. 5: SEM picture for experiment number 16

The effect of process parameters on tool wear: The effects of the axial depth of cut and feed per tooth on tool wear are shown in Fig. 4. The feed per tooth had a linear effect on tool wear, whereas the axial depth of cut had a quadratic effect. It is clear from the figure that the tool wear definitely increases for the increase in feed rate for all axial depths of cut was observed. For the cutting speed of 225 m/min, the tool-chip contact length is shorter, which causes the high mechanical stresses and cutting forces adjacent to the main cutting edge was concentrated. Due to generations of high cutting temperature, the cutting edge becomes to soften and the concentrated high cutting forces at the cutting edge lead to accelerate a tool wear (Liu *et al*., 2002). It can further be noted that in Fig. 5, the presence of adhering particle on the tool surface was observed in the experiment 16. The particle comes from the milled material and confirms the presence of the adhesion tool wear mechanism. The magnitude of flank wear widely varies reasonably the tool possess to sharp variation in stresses and temperature during machining.

The effect of process parameters on metal removal rate: The 3D surface graph, axial depth of cut versus feed per tooth in Fig. 6, shows that a significant mutual interaction occurs between feed per tooth and axial depth of cut for MRR as a response. Increase of MRR with the increase of feed per tooth for all the axial depth of cut. In general, general, the axial depth of cut determines the cutting edge to engage for removing the metal and feed per tooth ensures the cross-sectional area of uncut chip. Therefore, for low values of axial depth of cut and feed per tooth combines to give less metal removal. The reason is insufficient undeformed chip thickness produces fewer amounts of metal removal due to rubbing rather than efficient cutting (Gopalsamy *et al*., 2009a). While, the highest 0.8 mm axial depth of cut and 0.20 mm/tooth of cutting is very deeper to ensure maximum metal removal based on temperature generation at the tool-chip interface. Resulting from high temperature softens the work piece material enabling to facilitate the chip removal process more effectively with high level of feed per tooth and axial depth of cut.

Chip morphology: In hard milling, the removal of chips was a significant role to determine the desired surface finish and tool life. The cutting speed, work material hardness, undeformed chip thickness, tool rake

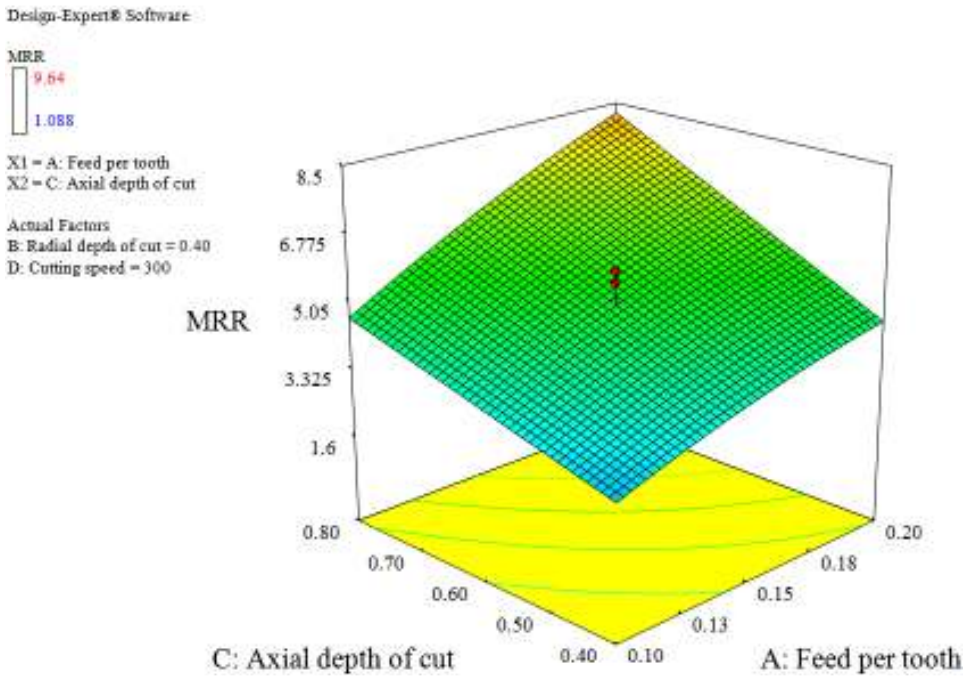

Fig. 6: 3D surface plot for MRR

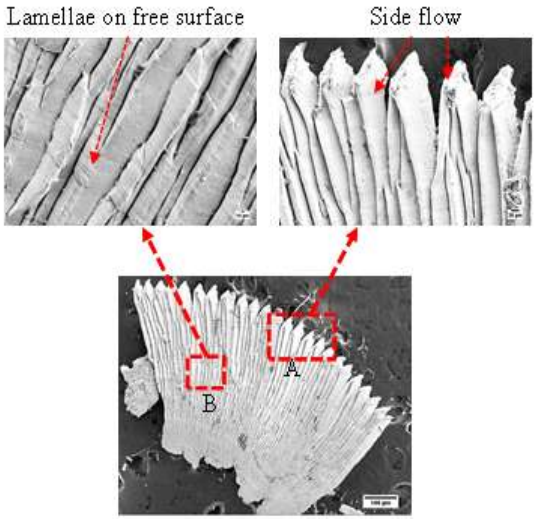

Fig. 7: Saw tooth chips observations for experiment 24

angle and flank wear are significantly influencing the chip morphology (Gopalsamy *et al*., 2009b). The chip formation is analyzed using scanning electron microscope for the collected chip of experiment 24 (0.15 mm/z feed rate, 0.40 mm radial depth of cut, 0.60 mm axial depth of cut and the cutting speed of 400 m/min). It is noticed from Fig. 7 that the typical homogeneous stabled saw-toothed chips are formed while machining of O1 tool steel. Visual examination suggests that a crack initiate on the work piece surface instead of plastic flow through the material during metal cutting. This crack, while releasing the stored energy acts a sliding plane for the material segments, allowing the chip segment to be forced out between the parting surfaces. Simultaneously, plastic deformation and heating of the work-piece material occur at the cutting tool edge. The crack will continue until cessation occurs in the limit of the material plastic deformation zone, which is facilitated by the high heat generated near the cut (Gopalsamy *et al*., 2009b). The side flows were observed in zone A due to piling up of a chip on cutting tool rake surface, the highly deformed material flowed downwards under the friction between cutting tool and chip and this depresses the deformed material to flow upwards. Further, increasing of cutting speed, the necessary thermal softening occurred. This makes the plastic deformation more concentrated at the inner end of the segment. Correspondingly, the side flows at higher cutting speed appear more abrupt form. In zone B, the outer portion of the uncut chip bends outwards under the squeeze of inner material. Localize deformation then is caused by the curvature of the free surface due to stress concentration there. This localized shear is regarded as the second initiation point of the concentrated shear band. The lamellae thickness is relatively constant and independent of undeformed chip thickness. The change in the structure of the free surface of continuous to saw tooth chip mainly depends on the work material hardness, cutting speed and feed (Su and Liu, 2013).

Multi-response optimization: Using derringer desirability function approach, a combination of input variables jointly optimizes a set of three responses by satisfying the requirements for each set in the response. The objective of this study is the minimization of

Table 4: Optimized hard milling parameters

Number	A	B	C	D	CT	TW	MRR	Desirability	
1	0.13	0.50	0.74	250	431.148	0.142	5.513	0.595	Selected
2	0.13	0.50	0.74	250	430.992	0.142	5.511	0.595	
3	0.13	0.50	0.74	250	431.476	0.143	5.534	0.595	
4	0.13	0.50	0.74	250	431.564	0.143	5.525	0.595	
5	0.13	0.50	0.74	250	430.890	0.142	5.485	0.595	
6	0.14	0.50	0.73	250	430.899	0.143	5.518	0.595	
7	0.13	0.50	0.74	250	432.161	0.143	5.542	0.595	
8	0.14	0.50	0.75	250	433.618	0.144	5.630	0.595	
9	0.13	0.50	0.73	250	427.809	0.140	5.339	0.594	
10	0.13	0.50	0.72	250	426.818	0.139	5.306	0.594	

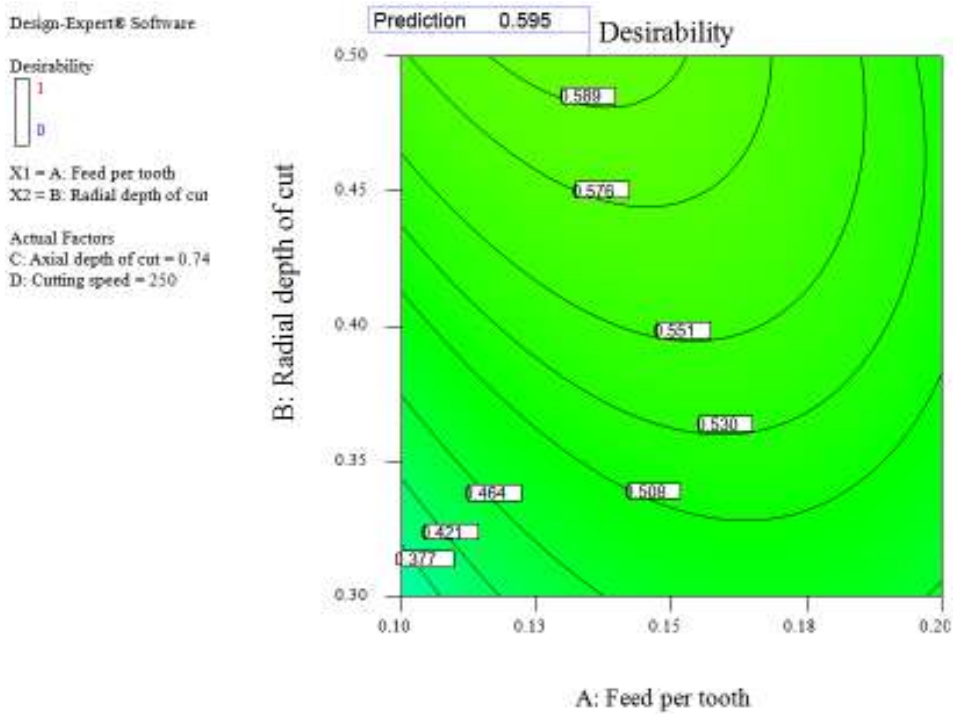

Fig. 8: Contour plot for overall desirability function

cutting temperature and tool wear with maximization of metal removal rate. The combination of the input variables leading to the optimum outputs can be identified by the Design Expert software. In response optimization, a measure of how the solution has satisfied the combined goals for all responses must be assured. The design variables used during an experimental study are: feed per tooth, radial depth of cut, axial depth of cut and cutting speed. The weight values assigned for all responses as one and each response can be assigned an importance relative to the other responses. Importance varies from the least important (+) a value of 1, to the most important (+++++) a value of 5. For each response, most importance was considered. When designing the individual desirability functions for each response, their lower and upper limits were set as maximum and minimum responses that could be obtained from the regression functions. Three responses have been optimized simultaneously using developed models, i.e.,

Table 5: Predicted and observed optimum values of responses

Response	Goal	Predicted	Observed	Error (%)
CT (°C)	Minimize	430.9652400	433.4200	0.56960
TW (mm)	Minimize	0.1422036	0.1501	5.55291
MRR (g/min)	Maximize	5.5014567	5.9168	7.54970

Eq. (4), (5) and (6). The best ten solutions obtained through the optimization are presented in Table 4. Always, the desired global solution for the maximum overall desirability is preferred. For the multi-response optimization problem, the optimal input parametric setting was selected with highest desirability of 0.595. The corresponding current optimal process parameter settings of 0. 13 mm/tooth feed, 0.50 mm of radial depth of cut, 0.74 mm of axial depth of cut and 250 m/min of cutting speed are considered. Finally; the contour plot of the overall desirability function was drawn as shown in Fig. 8. The near optimal region was located left-hand side approximately near the central region of the plot, which had a composite desirability

0.595 that gradually diminish towards right and left downwards.

Model verification: In the final step, a hard milling experiment based on the obtained optimal cutting conditions was conducted in order to verify the validity of the obtained optimal values. Table 5 shows the predicted and experimental responses at the optimal condition. As can be seen, the differences between the estimated and experimental responses are within the margin of 8%. The results are closely related to the data obtained from optimization analysis using desirability functions, indicating central-composite design incorporates with desirability functions could be effectively used to obtain the minimum value of CT, TW with a maximum value of MRR. Obviously, this confirms excellent reproducibility of the experiment conclusions.

CONCLUSION

In the present work, it was demonstrated the applicability of central composite design, response surface methodology and desirability function approach for modelling and multi-response optimization of a hard milling process. The results are summarized as follows:

- The predicted values match the experimental values reasonably well, with an R^2 of 0.98958 for CT, R^2 of 0.99749 for TW and R^2 of 0.96973 for MRR.
- The developed regression models and the obtained optimal cutting condition are valid within the experimental range as a region of interest.
- The optimal solution confirmed by experiment involves the following levels of factors from the multi-response optimization: Feed per tooth = 0.13 mm/z, radial depth of cut = 0.5 mm, axial depth of cut = 0.74 mm and cutting speed = 250 m/min.
- A thermal fatigue tool wear mechanism was characterized by the presence of fissures at higher cutting temperature in the worn tool.
- Stabled saw tooth chips were produced while hard milling of tool steel.
- The feed per tooth and axial depth of cut significantly influencing CT, TW and MRR.
- The CT majorly affects in the order of cutting speed, axial depth of cut, feed per tooth, the quadratic term of cutting speed and radial depth of cut.
- The most influential parameters on TW are identified as the feed per tooth, a quadratic term of axial depth of cut, cutting speed, a quadratic term of radial depth of cut and feed per tooth in order.
- The MRR was found to be more sensitive to an axial depth of cut, radial depth of cut, feed per tooth and cutting speed.
- The results obtained would be useful and serve as a technical database for mold and die manufacturing industries.

REFERENCES

ASM Handbook, 1991. Heat Treating. 10th Edn., Vol. 4, ASM International, pp: 387-424.

Cui, X., J. Zhao and X. Tian, 2012. Tool wear in high-speed face milling of AISI H13 steel. J. Eng. Manuf., 226: 1684-1693.

Cydas, U., 2010. Machinability evaluation in hard turning of AISI 4340 steel with different cutting tools using statistical techniques. J. Eng. Manuf., 224: 1043-1055.

Davim, J.P., 2011. Machining of Hard Materials. Springer-Verlag Ltd., London.

Derringer, G. and R. Suich, 1980. Simultaneous optimization of several response variables. J. Qual. Technol., 12(4): 214-219.

Ding, T., S. Zhang, Y. Wang and X. Zhu, 2010. Empirical models and optimal cutting parameters for cutting forces and surface roughness in hard milling of AISI H13 steel. Int. J. Adv. Manuf. Tech., 51: 45-55.

El-Wardany, T.I., H.A. Kishawy and M.A. Elbestawi, 2000. Surface integrity of die material in high speed hard machining-part 2: Microhardness variations and residual stresses. J. Manuf. Sci. Eng., 122: 632-640.

Escalona, P.M., N. Diaz and Z. Cassier, 2012. Prediction of tool wear mechanisms in face milling AISI 1045 steel. J. Mater. Eng. Perform., 21: 797-808.

Ghani, J.A., I.A. Choudhury and H.H. Masjuki, 2004. Performance of P10 TiN coated carbide tools when end milling AISI H13 tool steel at high cutting speed. J. Mater. Process. Technol., 153/154: 1062-1066.

Gopalsamy, B.M., B. Mondal and S. Ghosh, 2009a. Optimisation of machining parameters for hard machining: grey relational theory approach and ANOVA. Int. J. Adv. Manuf. Tech., 45: 1068-1086.

Gopalsamy, B.M., B. Mondal, S. Ghosh, K. Arntz and F. Klocke, 2009b. Investigations on hard machining of Impax Hi Hard tool steel. Int. J. Mater. Form., 2: 145-165.

Gopalsamy, B.M., B. Mondal, S. Ghosh, K. Arntz and F. Klocke, 2010. Experimental investigations while hard machining of DIEVAR tool steel (50 HRC). Int. J. Adv. Manuf. Tech., 51: 853-869.

Gu, J., G. Barber, S. Tung and R.J. Gu, 1999. Tool life and wear mechanism of uncoated and coated milling inserts. Wear, 225-229: 273-284.

Liu, Z.Q., X. Ai, H. Zhang, Z.T. Wang and Y. Wan, 2002. Wear patterns and mechanisms of cutting tools in high-speed face milling. J. Mater. Process. Tech., 126: 222-226.

Mativenga, P.T. and K.K.B. Hon, 2005. Wear and cutting forces in high-speed machining of H13 using physical vapour deposition coated carbide tools. J. Eng. Manuf., 219: 191-199.

Montgomery, D.C., 2012. Design and Analysis of Experiments. 8th Edn., Wiley, New York.

Okada, M., A. Hosokawa, R. Tanaka and T. Ueda, 2011. Cutting performance of PVD-coated carbide and CBN tools in hard milling. Int. J. Mach. Tool. Manu., 51: 127-132.

Palanisamy, P., I. Rajendran, S. Shanmugasundaram and R. Saravanan, 2006. Prediction of cutting force and temperature rise in the end-milling operation. J. Eng. Manuf., 220: 1577-1587.

Sato, M., T. Ueda and H. Tanaka, 2007. An experimental technique for the measurement of temperature on CBN tool face in end milling. Int. J. Mach. Tool Manu., 47: 2071-2076.

Siller, H.R., C. Vila, C.A. Rodríguez and J.V. Abellán, 2009. Study of face milling of hardened AISI D3 steel with a special design of carbide tools. Int. J. Adv. Manuf. Tech., 40: 12-25.

Su, G. and Z. Liu, 2013. Analytical and experimental study on formation of concentrated shear band of saw tooth chip in high-speed machining. Int. J. Adv. Manuf. Tech., 65: 1735-1740.

Toh, C.K., 2005. Comparison of chip surface temperature between up and down milling orientations in high speed rough milling of hardened steel. J. Mater. Process. Tech., 167: 110-118.